Journal of Applied Physics

Domain wall chirality reversal by interfacial engineering in Pt/Co/Pt based perpendicularly magnetized systems

Cite as: J. Appl. Phys. **133**, 023907 (2023); https://doi.org/10.1063/5.0117198
Submitted: 03 August 2022 • Accepted: 26 December 2022 • Published Online: 13 January 2023

Saikat Maji, Ankan Mukhopadhyay, Soubhik Kayal, et al.

Journal of Applied Physics ARTICLE scitation.org/journal/jap

Domain wall chirality reversal by interfacial engineering in Pt/Co/Pt based perpendicularly magnetized systems

Cite as: J. Appl. Phys. **133**, 023907 (2023); doi: 10.1063/5.0117198
Submitted: 3 August 2022 · Accepted: 26 December 2022 ·
Published Online: 13 January 2023

Saikat Maji, Ankan Mukhopadhyay, Soubhik Kayal, and P. S. Anil Kumar[a)]

AFFILIATIONS

Department of Physics, Indian Institute of Science, Bangalore 560012, India

[a)]**Author to whom correspondence should be addressed:** anil@iisc.ac.in

ABSTRACT

Heavy metal/ferromagnet interfaces in systems with perpendicular magnetic anisotropy (PMA) hosts chiral Néel wall with the assistance of interfacial Dzyaloshinskii–Moriya interaction (iDMI). We have investigated field induced domain wall motion in the creep regime to estimate the effective iDMI strength, D_{eff} of sputter-deposited Ta/Pt/Co/Pt and Ta/Pt/Co/Au/Pt thin films that exhibit PMA. Two similar Pt/Co interfaces on either side of the Co layer in the Ta/Pt/Co/Pt system lead to a small D_{eff} with a negative sign that supports the Néel type domain wall of right-handed chirality. Ultrathin Au layers of different thicknesses have been deposited at the top Co/Pt interface to introduce asymmetry around the Co layer and control the D_{eff}. Here, two interfaces (Pt/Co and Au/Co) of opposite iDMI polarity have been chosen to invert the domain wall chirality to the left-handed chirality instead of the right-handed chirality found in the Ta/Pt/Co/Pt system.

I. INTRODUCTION

Tuning the interfacial Dzyaloshiniskii–Moriya interaction (iDMI)[1–4] in heavy metal (HM)/ferromagnet (FM)/heavy metal (HM) and HM/FM/metal-oxide thin film systems with perpendicular magnetic anisotropy (PMA) has allured massive attention in the recent past because of their ability to construct next-generation high-density magnetic data storage devices[5,6] with lower power consumption. Structural inversion asymmetry at the HM/FM interface introduces iDMI in the FM layer that is known to stabilize chiral Néel walls[7–10] in PMA systems, magnetic skyrmions,[11,12] and many other spin textures. Spin-polarized current from heavy metal provides spin–orbit torque (SOT) that helps us to achieve high domain wall (DW) velocity[13–15] and current-induced magnetization reversal of the FM layer's magnetization with[15–18] or without[19–23] bias magnetic field in HM/FM/HM trilayers.

Several complicated methods[9,10,24–31] have been proposed to estimate the iDMI strength, D_{eff} of ultrathin magnetic films. Methods, which include electrical current, causes Joule heating. On the other hand, field induced domain wall motion (FIDWM) study proposed by Je *et al.*[32] is a straightforward and non-destructive method to calculate iDMI. In the FIDWM model, iDMI can be considered as an in-plane (IP) magnetic field (H_{DMI}), which is dominant inside the domain wall and the direction of H_{DMI} defines the chirality of Néel type domain walls. Je *et al.*[32] showed that a circular bubble domain nucleated in Pt/Co/Pt trilayers expands symmetrically in the radial direction when it is driven by only out of plane (OP) magnetic field (H_z). With the application of an in-plane (IP) magnetic field (H_x), in addition to H_z, the IP field can be added to H_{DMI} on one side and subtracted from H_{DMI} on the other side of the domain wall (DW) producing different domain wall velocities giving rise to the asymmetric expansion of bubble domain.[32,33] The H_x dependence of the domain wall velocity at a particular H_z is symmetric around H_{DMI} where the velocity becomes minimum. A small asymmetric contribution in velocity dependence has been confirmed in some studies due to chiral damping,[34] or tilt in the magnetization.[35,36] Precise tuning of D_{eff} has been achieved by introducing material asymmetry as reported in $Pt/Co/Au_xPt_{1-x}$ trilayers where iDMI increases gradually with an increase in x.[37] It has been observed that the interface quality[38,39] of Pt/Co plays a major role in iDMI interaction. In this work, asymmetric expansion of bubble domains in Ta/Pt/Co/Au/Pt multilayers with varying Au layer thickness has been studied to estimate iDMI strength, D_{eff}, and determine the DW chirality.

II. EXPERIMENTAL DETAILS

Ta(3 nm)/Pt(3 nm)/Co(0.4 nm)/Au(t nm)/Pt(1 nm) samples have been deposited using a d.c. magnetron sputtering system kept at a base pressure below 3×10^{-8} mbar where $x = 0$, 0.3, 0.5, and 0.7. Samples were deposited on an oxidized silicon wafer at room temperature with an Argon pressure 5×10^{-3} mbar. The average deposition rates for Ta, Pt, Co, and Au were 0.027, 0.038, 0.019, and 0.056 nm/s, respectively. The uniformity of the deposited films was ensured by rotating the substrate with a stepper motor at a rotation speed of 30 rpm. Room temperature magnetic characterizations were performed using the vibrating sample magnetometry (VSM) technique. FIDWM study has been carried out on all samples using a wide field differential Kerr microscopy (Evico-Magnetics) in the polar mode in presence of an OP magnetic field, H_z driven by a Kepco power supply (Model BOP 100-4ML provides maximum field up to 10 mT and minimum pulsewidth of 1 ms) and an IP biasing magnetic field, H_x driven by a polytronics power supply (Model BCS-100 provides maximum field up to 200 mT). To calculate domain wall velocity, at first, the sample was magnetized in $+z$ direction applying large $+H_z$. Then, a bubble domain was nucleated by applying a pulsed magnetic field in $-H_z$ of appropriate magnitude and pulsewidth (Δt). The domain image was captured by a CCD camera. A MATLAB program was used to determine the domain wall velocity from consecutive pulses. The detailed measurement technique is also described by Guddeti *et al.*[21]

III. RESULT AND DISCUSSION

A. Growth characterization

The thickness and interface roughness of individual layers present in each multilayer film were estimated performing x-ray reflectivity (XRR) measurements and fitting XRR data using ReMagX software[40] (shown in Fig. 1). The fitting results that are presented in Table I show a high quality of the interfaces in the samples.

B. Magnetic characterization

The PMA behavior has been confirmed from the hysteresis loop of all the samples at room temperature. The magnetization data have been obtained using vibrating sample magnetometry (VSM) for both applied OP and IP magnetic fields (Fig. 2). The effective anisotropy energy, $K_{\text{eff}} = M_S \times H_K/2$, and the domain wall width, $\lambda = \sqrt{A/K_{\text{eff}}}$, was calculated from the VSM data and is presented in Fig. 3, where M_s, H_K, and A stands for saturation magnetization, anisotropy field, and exchange stiffness constant, respectively. The value of exchange stiffness constant, $A = 16$ pJ/m

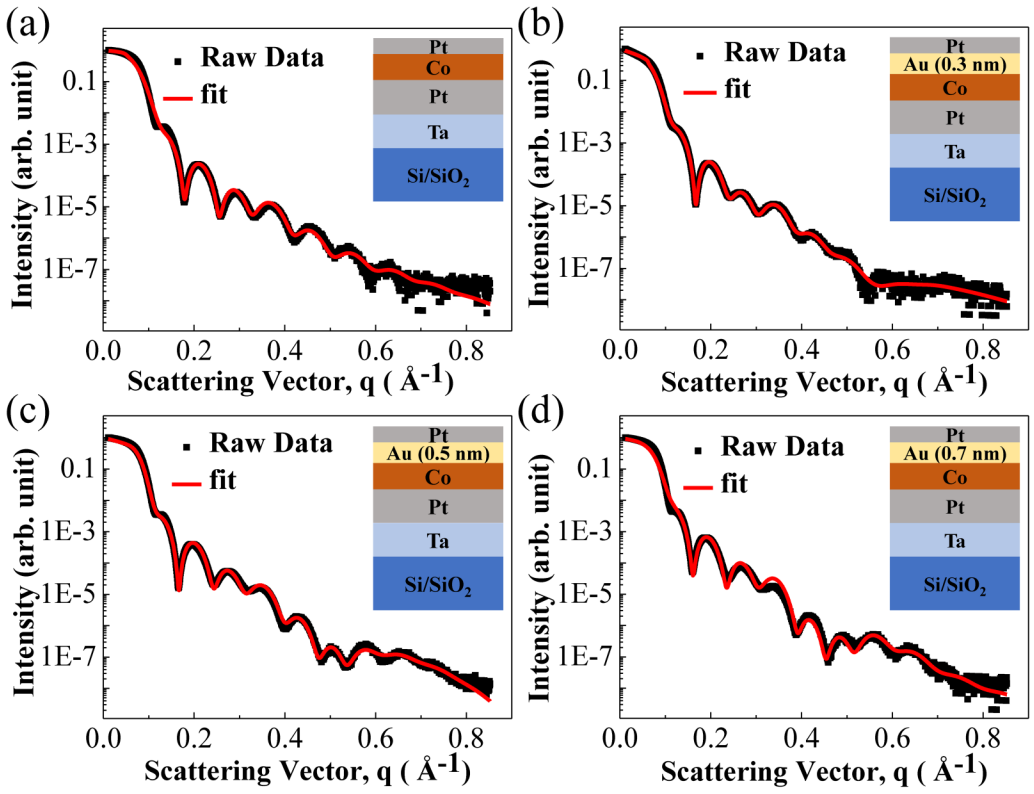

FIG. 1. XRR data fitted with ReMagX software for sample (a) Au (0 nm), (b) Au (0.3 nm), (c) Au (0.5 nm), and (d) Au (0.7 nm).

TABLE I. Thickness t and roughness σ in nm of all the layers in each multilayer.

Multilayer	$\sigma_{SiO_2/Ta}$	t_{Ta}	$\sigma_{Ta/Pt}$	t_{Pt}	$\sigma_{Pt/Co}$	t_{Co}	$\sigma_{Co/Pt}$	t_{Pt}	$\sigma_{Pt/air}$	…	…
Au 0.0	0.42	3.71	0.62	2.91	0.70	0.38	0.20	0.90	0.46	…	…
Multilayer	$\sigma_{SiO_2/Ta}$	t_{Ta}	$\sigma_{Ta/Pt}$	t_{Pt}	$\sigma_{Pt/Co}$	t_{Co}	$\sigma_{Co/Au}$	t_{Au}	$\sigma_{Au/Pt}$	t_{Pt}	$\sigma_{Pt/air}$
Au 0.3	0.52	3.67	0.57	2.82	0.50	0.41	0.16	0.30	0.42	0.90	0.46
Au 0.5	0.44	3.45	0.59	2.68	0.30	0.38	0.31	0.47	0.40	0.90	0.31
Au 0.7	0.40	3.55	0.69	2.65	0.20	0.39	0.35	0.70	0.49	0.92	0.43

was taken from the literature[41] for a similar system. The increment of the K_{eff} with the increase in Au thickness suggests a strong PMA behavior in these samples.

C. Field induced domain wall motion

To obtain D_{eff} from the FIDWM technique, we study the velocity of DWs driven by the OP field, H_z, in the presence of the IP bias field, H_x in the creep regime. The IP bias field primarily modulates the domain wall energy of a bubble domain present in our samples and an asymmetric bubble expansion is observed. In the creep regime, the DW velocity, v can be expressed as[34,42,43]

$$v = v_0 \exp\left[-\zeta(\mu_0 H_z)^{-1/4}\right], \tag{1}$$

where v_0 is the characteristic velocity and ζ is a scaling coefficient related to total IP field present in the system that comprises of both effective IP field due to iDMI, H_{DMI} and applied IP field, H_x. ζ can be expressed as

$$\zeta = \zeta_0[\sigma(H_x)/\sigma_0]^{1/4}, \tag{2}$$

where ζ_0 is a scaling coefficient, $\sigma(H_x)$ is the domain wall energy density expressed as a function of H_x, and σ_0 is the energy density of Bloch wall. The domain wall energy density can be expressed as[7,44]

$$\sigma(H_x) = \sigma_0 - \frac{\pi^2 \lambda \mu_0 M_s^2}{8K_D}(H_x + H_{DMI})^2. \tag{3}$$

where $K_D = (N_x \mu_0 M_s^2)/2$ is the DW energy density[45] and $N_x = (ln(2)t_{Co})/(\pi\lambda)$ is the DW demagnetization factor. When H_{DMI} is small enough such that $|H_x + H_{DMI}| < 4K_D/\pi\mu_0 M_s$, DW remains in Bloch state and Eq. (3) is valid. If H_{DMI} is large enough such that $|H_x + H_{DMI}| > 4K_D/\pi\mu_0 M_s$, DW transforms into the Néel state from the Bloch state. The DW energy density for a Néel wall as described in Eq. (4) is needed to be used instead of Eq. (3). The magnetization inside the Néel wall rotates in a plane perpendicular to the DW plane. Depending on the sense of rotation, Néel walls can exhibit left-handed or right-handed chirality. The direction of H_{DMI} fixes the chirality of the Néel wall. The DW energy density for the Néel wall is given as[7,32,44]

$$\sigma(H_x) = \sigma_0 - 2\lambda K_D - \pi\lambda\mu_0 M_s|H_x + H_{DMI}|. \tag{4}$$

In PMA systems, large iDMI stabilizes the chiral Néel wall. Substituting the energy density for the Néel wall into Eqs. (2) and (1), the domain wall velocities obtained as a function of H_x

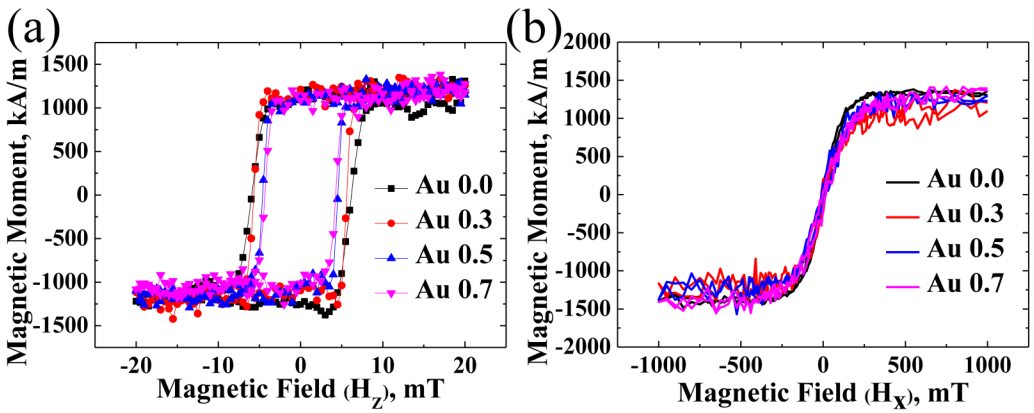

FIG. 2. Hysteresis plot for applied (a) out of plane magnetic field, H_z and (b) in-plane magnetic field, H_x.

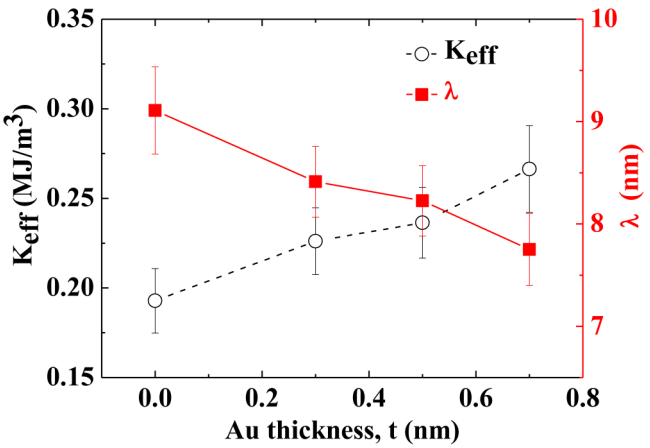

FIG. 3. The anisotropy energy, K_{eff} (dashed line), and domain wall thickness, λ (solid line), as a function of Au thickness (t).

have a velocity minimum at $H_x = H_{DMI}$. This method can be employed to measure the H_{DMI} experimentally.

In the absence of the IP field ($H_x = 0$), the velocity is the same throughout the DW since the domain wall energy is also the same. Thus, the symmetric expansion of DWs has been seen in the presence of only pulsed H_z, which is shown in Fig. 4(a). However, in the presence of an IP field ($H_x \neq 0$), the DW energy gets modified according to Eq. (4) due to the chiral nature of the Néel wall. The modification of DW energy leads to asymmetric expansion of the domain wall. To determine H_{DMI}, the DW velocity of the left wall (LW) with respect to H_x has been extracted for different H_z and fitted with Eq. (1) as described by Hrabec *et al.*[46] The left wall velocity for a fixed H_z is shown and the fitted curve using the creep law is shown in Fig. 4(b). The velocity minima were obtained at $H_x = H_{min}$ after fitting. The H_{min} for different H_z has been found, and the average value is denoted as H_{DMI}. The contour plot of DW velocity as a function of H_z and H_x is also presented in Fig. 5, where H_{DMI} is indicated with a dotted line. The H_{DMI} sign reverses with the insertion of Au at the top Co/Pt interface.

The asymmetric expansion of bubble domains in the presence of H_x reveals the chirality of domain walls. The schematic of magnetization configuration inside DW has been presented in Fig. 6 along with the asymmetric DW expansion. In Ta/Pt/Co/Pt sample [Fig. 6(a)], the right wall of the nucleated bubble domain has a faster velocity than the left wall, indicating that the right wall has a lower DW energy. As per Eq. (4), the DW energy lowers when H_{DMI} and H_x are directed in the same direction. The possible magnetization configuration (as shown in Fig. 6) can be predicted knowing the direction of H_{DMI}. The magnetization configuration unveils that the Ta/Pt/Co/Pt system has DW with right-handed chirality. When an ultrathin layer of Au is introduced at the top Co/Pt interface, the right wall expands slower than the left wall, suggesting H_{DMI} directs opposite to the H_x inside the right wall. The magnetization configuration in Ta/Pt/Co/Au/Pt samples [Figs. 6(b)–6(d)] shows that these samples host DW with left-handed chirality. The FIDWM study has been performed to estimate H_{DMI} in epitaxial $Pt/Co/Au_xPt_{1-x}$ trilayers[37] for x = 0, 0.5, 1. The top layer in $Pt/Co/Au_{0.5}Pt_{0.5}$ is an alloy achieved using the co-sputtering technique. Pt/Co/Pt system shows negligibly small H_{DMI}, Pt/Co/Au shows a higher H_{DMI} and $Pt/Co/Au_{0.5}Pt_{0.5}$ have H_{DMI} of intermediate strength. The H_{DMI} stabilizes the domain wall with left-handed chirality in all these systems. On the contrary, in our study, the Ta/Pt/Co/Pt system stabilizes the domain wall with right-handed chirality. The domain wall chirality reverses to left-handed in Ta/Pt/Co/Au/Pt multilayers.

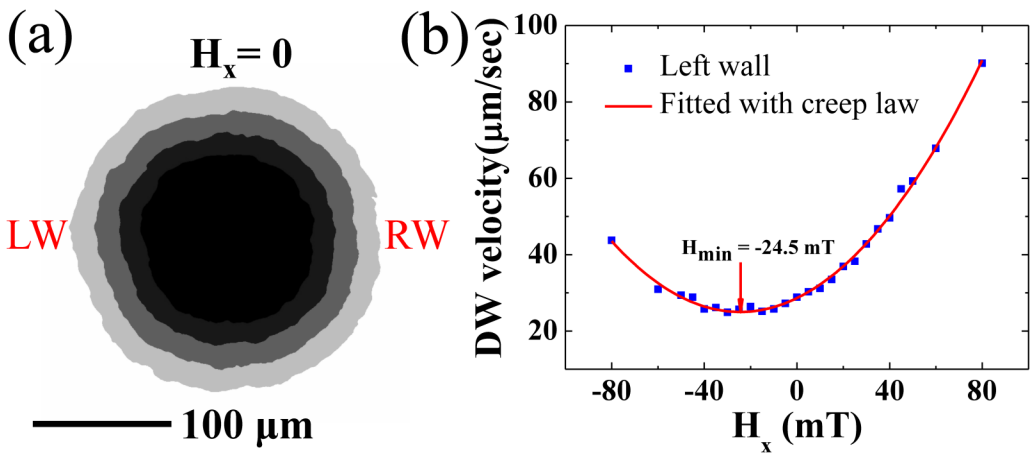

FIG. 4. (a) Symmetric expansion of a nucleated bubble domain for pulsed $H_z = -7.5$ mT of pulsewidth, $\Delta t = 200$ ms and an applied in-plane magnetic field, $H_x = 0$. The left and right wall has been labeled with LW and RW, respectively. (b) Domain wall velocity as a function of H_x for Ta/Pt/Co/Pt system is plotted (squares) and fitted with creep law (solid line). The minimum of the velocity has been indicated with H_{min}.

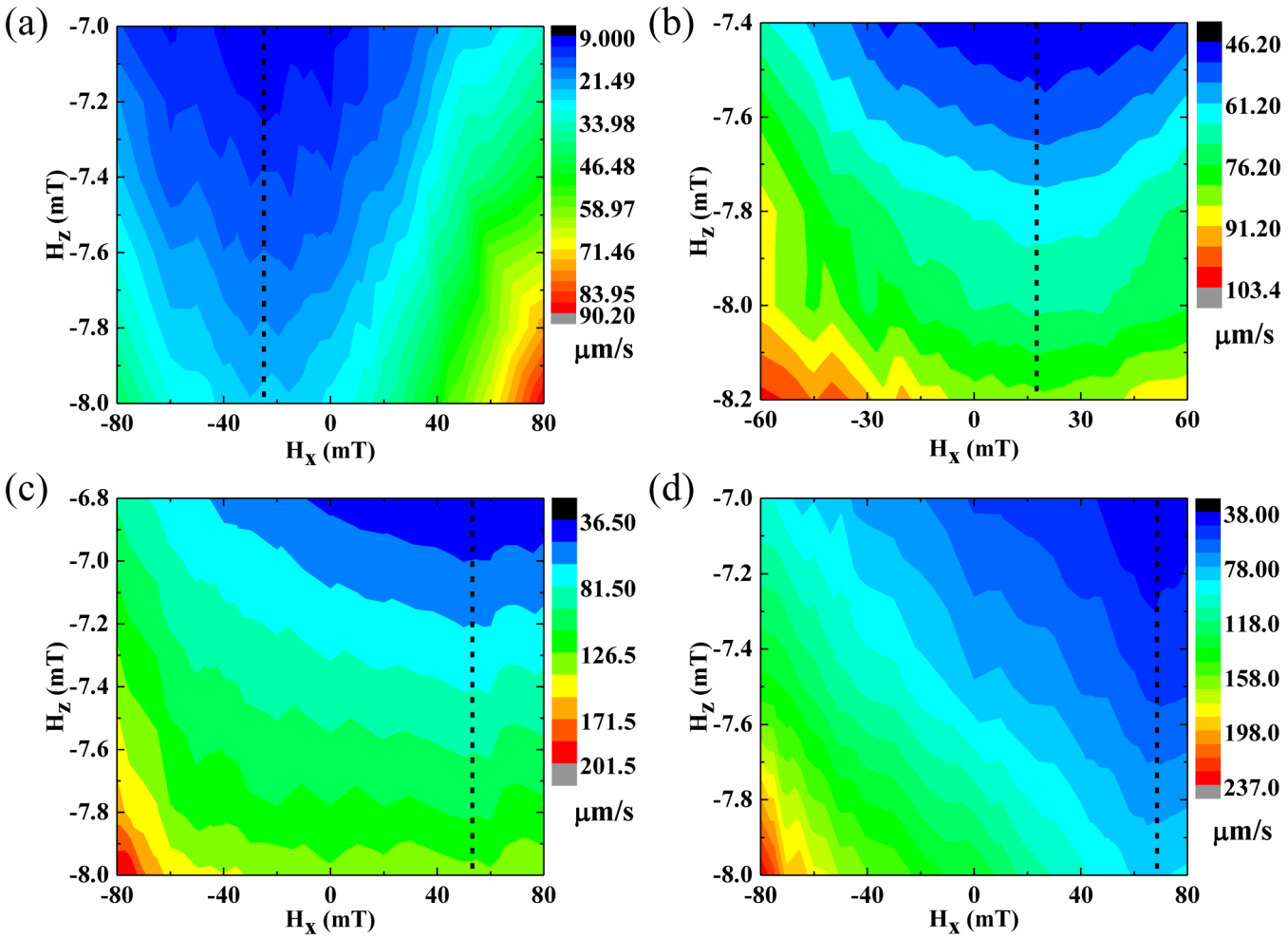

FIG. 5. Contour plot of left wall velocity as a function of H_x and H_z for Au thickness (a) 0 nm, (b) 0.3 nm, (c) 0.5 nm, and (d) 0.7 nm. The colorbar represents the domain wall velocity in μm/s. The H_{DMI} is indicated with black dotted line in each plot.

The D_{eff} value has been estimated using the formula $D_{\text{eff}} = \mu_0 H_{DMI} M_s \lambda$[7,32] and displayed in Fig. 7. D_{eff} in the HM/FM/HM system consists of iDMI contribution from both the bottom HM/FM and top FM/HM interface. Individual Pt/Co interface produces positive iDMI[47] as shown in Fig. 8(a). Also, the iDMI depends on interface roughness or intermixing.[39,48] In the Pt/Co/Pt system, iDMI of bottom Pt/Co counters top Co/Pt interface [Fig. 8(c)]. It has been observed that D_{eff} becomes negligibly small for an epitaxial Pt/Co/Pt system.[46] Two similar interfaces on either side of Co produce a resultant iDMI that is small in magnitude. The iDMI strength, $D_{\text{eff}} = -0.29\,\text{mJ/m}^2$, was obtained for such a symmetric Ta/Pt/Co/Pt system. This small value of D_{eff} can be attributed to the difference between the interface roughness of the two Pt/Co interface. In Ta/Pt/Co/Au/Pt systems, an ultrathin layer of Au was inserted at the top Co/Pt interface to introduce asymmetry around Co layer. The D_{eff} enhanced as more asymmetry to the Ta/Pt/Co/Pt system was introduced by increasing the thickness of the Au layer. The maximum iDMI strength ($D_{\text{eff}} = 0.60\,\text{mJ/m}^2$) was achieved for the sample having highest degree of asymmetry (Au thickness, $t = 0.7$ nm). In addition, for the samples with an Au layer, the iDMI strength was inverted. Pt/Co and Au/Co have opposite polarity of iDMI as predicted theoretically.[47,49,50] The iDMI configuration of the Au/Co interface has been shown in Fig. 8(b). The sign of iDMI at the Au/Co interface is flipped due to the inversion of stacking geometry from Au/Co to Co/Au in order to produce Pt/Co/Au trilayer [see Fig. 8(d)]. Unlike the Ta/Pt/Co/Pt system, the combined effect of bottom Pt/Co and top Co/Au interfaces with the same iDMI polarity reverses the effective iDMI of Ta/Pt/Co/Au/Pt multilayers.

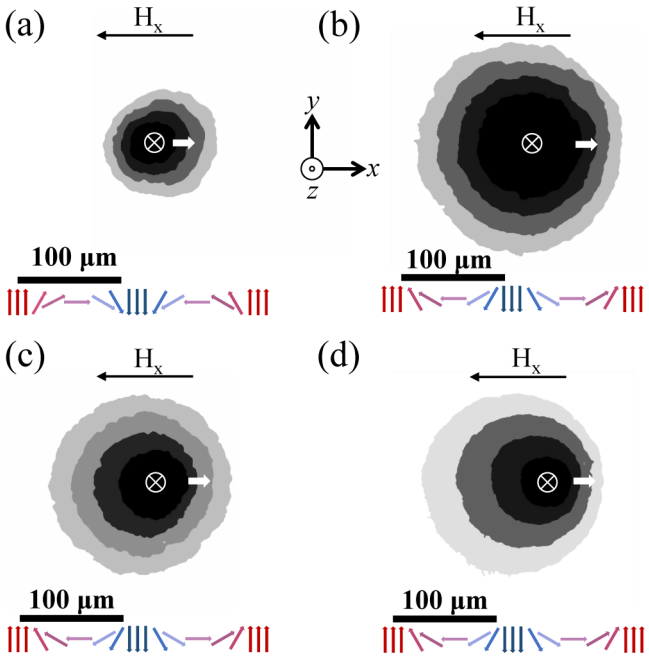

FIG. 6. Asymmetric expansion of bubble domain at an in-plane magnetic field, $H_x = 30$ mT. (a) Au ($t = 0$ nm), (b) Au ($t = 0.3$ nm), (c) Au ($t = 0.5$ nm), and (d) Au ($t = 0.7$ nm) after application of pulsed $H_z = -7.8$ mT of $\Delta t = 400$ ms, $H_z = -7.8$ mT of $\Delta t = 260$ ms, $H_z = -7.8$ mT of $\Delta t = 200$ ms and $H_z = -8.0$ mT of $\Delta t = 210$ ms, respectively. Each image contains four successive pulses. A different color shade is provided to distinguish the domain expansion after each pulse. The magnetization of the nucleated bubble is along $-z$ direction as pointed by the cross at the center of the domain. The schematic of magnetization configuration inside the domain wall (xz plane) is shown under each image. The domain wall velocity along x-direction is indicated with white arrow. Neél walls with right-handed chirality were found in Au (0 nm) sample, whereas left-handed Neél walls were observed after the introduction of the Au layer with thickness ($t = 0.3$, 0.5, 0.7 nm) at Co/Pt interface.

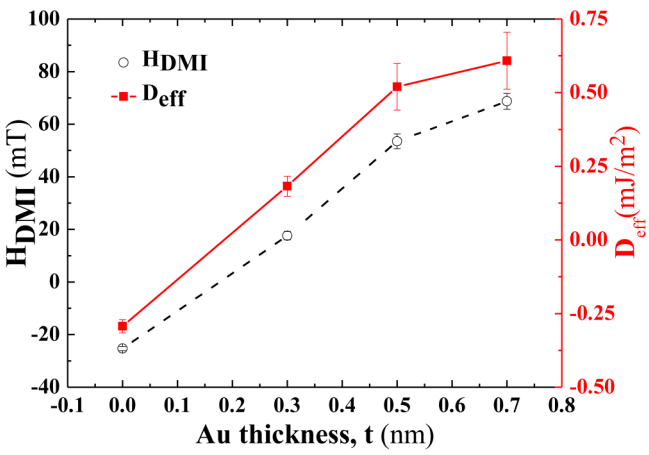

FIG. 7. Effective in-plane field of iDMI, H_{DMI} (circles) and iDMI strength, D_{eff} (squares) as a function of Au layer thickness. iDMI sign reverses with the introduction of the ultrathin layer of Au.

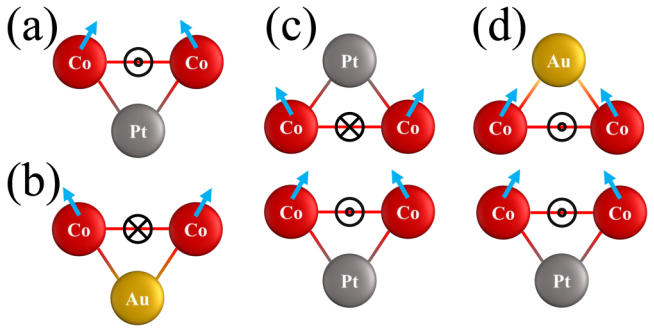

FIG. 8. Schematic diagram of iDMI configuration. The direction of iDMI points either into the paper or out of the plane of the paper. The magnetization has been represented with the arrows attached to Co. (a) Pt/Co interface with positive iDMI. (b) Au/Co interface with negative iDMI.[47] (c) Pt/Co/Pt system involves iDMI contribution from both bottom Pt/Co and top Co/Pt interfaces that cancels each other. (d) In Pt/Co/Au multilayer, bottom Pt/Co interface and top Co/Au interface have same iDMI polarity that adds up to produce enhanced iDMI.

IV. CONCLUSIONS

We deposited Ta/Pt/Co/Au/Pt multilayer thin films of varying Au thickness using the sputter deposition technique and characterized them with proper thickness and interface roughness fitting x-ray reflectivity data. We determined the magnetic properties using a Vibrating sample magnetometer. We have studied the field-driven asymmetric expansion of the bubble domain in presence of an in-plane bias magnetic field to determine the effective strength of the interfacial Dzyaloshinskii–Moriya interaction (iDMI). Ta/Pt/Co/Pt multilayer exhibits negative iDMI with the Néel type domain wall of right-handed chirality. We can alter the chirality of the Néel wall from right-handed to left-handed as effective iDMI strength is reversed with the introduction of an ultrathin layer of Au at the top Co/Pt interface. This study demonstrates that two different HM/FM (Pt/Co and Au/Co) interfaces having opposite polarity of iDMI can be used to achieve higher iDMI strength as well as reverse the chirality of the domain wall. Also, the variation of iDMI strength as a function of the Au layer provides precise control over the iDMI in HM/FM/HM multilayers.

ACKNOWLEDGMENTS

We acknowledge the fruitful discussion we had on Dzyaloshinskii–Moriya interaction with Professor R. A. Duine and Dr. B. Ravi Kumar. We also acknowledge National Nano-fabrication Center (NNFC), Centre for Nano Science and Engineering (CeNSE) for clean-room facility and Micro-Nano Characterization Facility (MNCF), CeNSE for measurement facilities. S.M. and A.M. would like to acknowledge the Ministry of Education (MoE), India, and S.K. would like to thank the Council of Scientific and Industrial Research (CSIR) for the research fellowship. P.S.A.K. gratefully acknowledges DST Nano Mission for financial support.

AUTHOR DECLARATIONS

Conflict of Interest

The authors have no conflicts to disclose.

Author Contributions

Saikat Maji: Conceptualization (equal); Data curation (lead); Formal analysis (lead); Investigation (lead); Methodology (lead); Writing – original draft (equal). **Ankan Mukhopadhyay:** Data curation (equal); Formal analysis (equal); Investigation (equal); Methodology (equal); Writing – review & editing (equal). **Soubhik Kayal:** Data curation (equal); Formal analysis (equal); Investigation (equal); Methodology (equal); Writing – review & editing (equal). **P. S. Anil Kumar:** Funding acquisition (lead); Project administration (lead); Supervision (lead); Writing – review & editing (lead).

DATA AVAILABILITY

The data that support the findings of this study are available from the corresponding author upon reasonable request.

REFERENCES

[1]I. Dzyaloshinsky, "A thermodynamic theory of "weak" ferromagnetism of antiferromagnetics," J. Phys. Chem. Solids **4**, 241–255 (1958).
[2]T. Moriya, "Anisotropic superexchange interaction and weak ferromagnetism," Phys. Rev. **120**, 91–98 (1960).
[3]T. Moriya, "New mechanism of anisotropic superexchange interaction," Phys. Rev. Lett. **4**, 228–230 (1960).
[4]A. Crépieux and C. Lacroix, "Dzyaloshinsky-Moriya interactions induced by symmetry breaking at a surface," J. Magn. Magn. Mater. **182**, 341–349 (1998).
[5]S. S. Parkin, M. Hayashi, and L. Thomas, "Magnetic domain-wall racetrack memory," Science **320**, 190–194 (2008).
[6]A. Fert, V. Cros, and J. Sampaio, "Skyrmions on the track," Nat. Nanotechnol. **8**, 152–156 (2013).
[7]A. Thiaville, S. Rohart, É. Jué, V. Cros, and A. Fert, "Dynamics of Dzyaloshinskii domain walls in ultrathin magnetic films," Europhys. Lett. **100**, 57002 (2012).
[8]K.-W. Kim, H.-W. Lee, K.-J. Lee, and M. D. Stiles, "Chirality from interfacial spin-orbit coupling effects in magnetic bilayers," Phys. Rev. Lett. **111**, 216601 (2013).
[9]S. Emori, U. Bauer, S.-M. Ahn, E. Martinez, and G. S. Beach, "Current-driven dynamics of chiral ferromagnetic domain walls," Nat. Mater. **12**, 611–616 (2013).
[10]K.-S. Ryu, L. Thomas, S.-H. Yang, and S. Parkin, "Chiral spin torque at magnetic domain walls," Nat. Nanotechnol. **8**, 527–533 (2013).
[11]W. Jiang, P. Upadhyaya, W. Zhang, G. Yu, M. B. Jungfleisch, F. Y. Fradin, J. E. Pearson, Y. Tserkovnyak, K. L. Wang, O. Heinonen, and S. G. Te Velthuis, "Blowing magnetic skyrmion bubbles," Science **349**, 283–286 (2015).
[12]O. Boulle, J. Vogel, H. Yang, S. Pizzini, D. de Souza Chaves, A. Locatelli, T. O. Menteş, A. Sala, L. D. Buda-Prejbeanu, O. Klein, and M. Belmeguenai, "Room-temperature chiral magnetic skyrmions in ultrathin magnetic nanostructures," Nat. Nanotechnol. **11**, 449–454 (2016).
[13]T. A. Moore, I. Miron, G. Gaudin, G. Serret, S. Auffret, B. Rodmacq, A. Schuhl, S. Pizzini, J. Vogel, and M. Bonfim, "High domain wall velocities induced by current in ultrathin Pt/Co/AlO_x wires with perpendicular magnetic anisotropy," Appl. Phys. Lett. **93**, 262504 (2008).
[14]I. M. Miron, T. Moore, H. Szambolics, L. D. Buda-Prejbeanu, S. Auffret, B. Rodmacq, S. Pizzini, J. Vogel, M. Bonfim, A. Schuhl, and G. Gaudin, "Fast current-induced domain-wall motion controlled by the Rashba effect," Nat. Mater. **10**, 419–423 (2011).
[15]P. Haazen, E. Murè, J. Franken, R. Lavrijsen, H. Swagten, and B. Koopmans, "Domain wall depinning governed by the spin Hall effect," Nat. Mater. **12**, 299–303 (2013).
[16]C. Onur Avci, K. Garello, I. Mihai Miron, G. Gaudin, S. Auffret, O. Boulle, and P. Gambardella, "Magnetization switching of an MgO/Co/Pt layer by in-plane current injection," Appl. Phys. Lett. **100**, 212404 (2012).
[17]L. Liu, O. J. Lee, T. J. Gudmundsen, D. C. Ralph, and R. A. Buhrman, "Current-induced switching of perpendicularly magnetized magnetic layers using spin torque from the spin Hall effect," Phys. Rev. Lett. **109**, 096602 (2012).
[18]R. M. Rowan-Robinson, A. Hindmarch, and D. Atkinson, "Efficient current-induced magnetization reversal by spin-orbit torque in Pt/Co/Pt," J. Appl. Phys. **124**, 183901 (2018).
[19]G. Yu, P. Upadhyaya, Y. Fan, J. G. Alzate, W. Jiang, K. L. Wong, S. Takei, S. A. Bender, L.-T. Chang, Y. Jiang, and M. Lang, "Switching of perpendicular magnetization by spin–orbit torques in the absence of external magnetic fields," Nat. Nanotechnol. **9**, 548–554 (2014).
[20]V. M. P. K. R. Ganesh and P. S. A. Kumar, "Spin Hall effect mediated current-induced deterministic switching in all-metallic perpendicularly magnetized Pt/Co/Pt trilayers," Phys. Rev. B **96**, 104412 (2017).
[21]S. Guddeti, A. K. Gopi, and P. S. Anil Kumar, "Effect of tilted magnetic anisotropy on the deterministic current-induced magnetization reversal in quasi-perpendicularly magnetized Ta/Pt/CoFeB/Pt multilayers," IEEE Trans. Magn. **54**, 1–5 (2018).
[22]B. Cui, H. Wu, D. Li, S. A. Razavi, D. Wu, K. L. Wong, M. Chang, M. Gao, Y. Zuo, L. Xi, and K. L. Wang, "Field-free spin–orbit torque switching of perpendicular magnetization by the Rashba interface," ACS Appl. Mater. Interfaces **11**, 39369–39375 (2019).
[23]S. Kayal, S. Maji, A. Mukhopadhyay, and P. Anil Kumar, "Enhancing the spin-orbit torque efficiency in Pt/CoFeB/Pt based perpendicularly magnetized system," J. Magn. Magn. Mater. **558**, 169499 (2022).
[24]Y.-K. Park, D.-Y. Kim, J.-S. Kim, Y.-S. Nam, M.-H. Park, H.-C. Choi, B.-C. Min, and S.-B. Choe, "Experimental observation of the correlation between the interfacial Dzyaloshinskii–Moriya interaction and work function in metallic magnetic trilayers," NPG Asia Mater. **10**, 995–1001 (2018).
[25]S. Meckler, N. Mikuszeit, A. Preßler, E. Y. Vedmedenko, O. Pietzsch, and R. Wiesendanger, "Real-space observation of a right-rotating inhomogeneous cycloidal spin spiral by spin-polarized scanning tunneling microscopy in a triple axes vector magnet," Phys. Rev. Lett. **103**, 157201 (2009).
[26]M. Belmeguenai, J.-P. Adam, Y. Roussigné, S. Eimer, T. Devolder, J.-V. Kim, S. M. Cherif, A. Stashkevich, and A. Thiaville, "Interfacial Dzyaloshinskii-Moriya interaction in perpendicularly magnetized Pt/Co/AlO_x ultrathin films measured by Brillouin light spectroscopy," Phys. Rev. B **91**, 180405 (2015).
[27]H. T. Nembach, J. M. Shaw, M. Weiler, E. Jué, and T. J. Silva, "Linear relation between Heisenberg exchange and interfacial Dzyaloshinskii–Moriya interaction in metal films," Nat. Phys. **11**, 825–829 (2015).
[28]G. Chen, T. Ma, A. T. N'Diaye, H. Kwon, C. Won, Y. Wu, and A. K. Schmid, "Tailoring the chirality of magnetic domain walls by interface engineering," Nat. Commun. **4**, 1–6 (2013).
[29]K. Di, V. L. Zhang, H. S. Lim, S. C. Ng, M. H. Kuok, J. Yu, J. Yoon, X. Qiu, and H. Yang, "Direct observation of the Dzyaloshinskii-Moriya interaction in a Pt/Co/Ni film," Phys. Rev. Lett. **114**, 047201 (2015).
[30]A. K. Chaurasiya, A. Kumar, R. Gupta, S. Chaudhary, P. K. Muduli, and A. Barman, "Direct observation of unusual interfacial Dzyaloshinskii-Moriya interaction in graphene/NiFe/Ta heterostructures," Phys. Rev. B **99**, 035402 (2019).
[31]A. Kumar, A. K. Chaurasiya, N. Chowdhury, A. K. Mondal, R. Bansal, A. Barvat, S. P. Khanna, P. Pal, S. Chaudhary, A. Barman, and P. K. Muduli, "Direct measurement of interfacial Dzyaloshinskii–Moriya interaction at the $MoS_2/Ni_{80}Fe_{20}$ interface," Appl. Phys. Lett. **116**, 232405 (2020).
[32]S.-G. Je, D.-H. Kim, S.-C. Yoo, B.-C. Min, K.-J. Lee, and S.-B. Choe, "Asymmetric magnetic domain-wall motion by the Dzyaloshinskii-Moriya interaction," Phys. Rev. B **88**, 214401 (2013).

[33]K.-W. Moon, D.-H. Kim, S.-C. Yoo, S.-G. Je, B. S. Chun, W. Kim, B.-C. Min, C. Hwang, and S.-B. Choe, "Magnetic bubblecade memory based on chiral domain walls," Sci. Rep. **5**, 1–5 (2015).
[34]D.-H. Kim, D.-Y. Kim, S.-C. Yoo, B.-C. Min, and S.-B. Choe, "Universality of Dzyaloshinskii-Moriya interaction effect over domain-wall creep and flow regimes," Phys. Rev. B **99**, 134401 (2019).
[35]A. Mukhopadhyay, S. Maji, and P. A. Kumar, "Asymmetric magnetic domain wall motion in quasi-perpendicularly magnetized Pt/Co/Pt trilayer with interfacial Dzyaloshinskii-Moriya interaction," J. Magn. Magn. Mater. **537**, 168125 (2021).
[36]S. Kayal, S. Maji, A. Mukhopadhyay, and P. Anil Kumar, "Asymmetric magnetic domain wall motion under lateral and normal space inversion asymmetry with interfacial Dzyaloshinskii–Moriya interaction," J. Magn. Magn. Mater. **551**, 168993 (2022).
[37]K. Shahbazi, A. Hrabec, S. Moretti, M. B. Ward, T. A. Moore, V. Jeudy, E. Martinez, and C. H. Marrows, "Magnetic properties and field-driven dynamics of chiral domain walls in epitaxial $Pt/Co/Au_xPt_{1-x}$ trilayers," Phys. Rev. B **98**, 214413 (2018).
[38]R. Lavrijsen, D. M. F. Hartmann, A. van den Brink, Y. Yin, B. Barcones, R. A. Duine, M. A. Verheijen, H. J. M. Swagten, and B. Koopmans, "Asymmetric magnetic bubble expansion under in-plane field in Pt/Co/Pt: Effect of interface engineering," Phys. Rev. B **91**, 104414 (2015).
[39]A. W. J. Wells, P. M. Shepley, C. H. Marrows, and T. A. Moore, "Effect of interfacial intermixing on the Dzyaloshinskii-Moriya interaction in Pt/Co/Pt," Phys. Rev. B **95**, 054428 (2017).
[40]S. Macke and E. Goering, "Magnetic reflectometry of heterostructures," J. Phys.: Condens. Matter **26**, 363201 (2014).
[41]C. Eyrich, W. Huttema, M. Arora, E. Montoya, F. Rashidi, C. Burrowes, B. Kardasz, E. Girt, B. Heinrich, O. Mryasov, and M. From, "Exchange stiffness in thin film co alloys," J. Appl. Phys. **111**, 07C919 (2012).
[42]S. Lemerle, J. Ferré, C. Chappert, V. Mathet, T. Giamarchi, and P. Le Doussal, "Domain wall creep in an Ising ultrathin magnetic film," Phys. Rev. Lett. **80**, 849–852 (1998).
[43]P. Chauve, T. Giamarchi, and P. Le Doussal, "Creep and depinning in disordered media," Phys. Rev. B **62**, 6241–6267 (2000).
[44]M. Heide, G. Bihlmayer, and S. Blügel, "Dzyaloshinskii-Moriya interaction accounting for the orientation of magnetic domains in ultrathin films: Fe/W(110)," Phys. Rev. B **78**, 140403 (2008).
[45]S. Tarasenko, A. Stankiewicz, V. Tarasenko, and J. Ferré, "Bloch wall dynamics in ultrathin ferromagnetic films," J. Magn. Magn. Mater. **189**, 19–24 (1998).
[46]A. Hrabec, N. A. Porter, A. Wells, M. J. Benitez, G. Burnell, S. McVitie, D. McGrouther, T. A. Moore, and C. H. Marrows, "Measuring and tailoring the Dzyaloshinskii-Moriya interaction in perpendicularly magnetized thin films," Phys. Rev. B **90**, 020402 (2014).
[47]H. Yang, O. Boulle, V. Cros, A. Fert, and M. Chshiev, "Controlling Dzyaloshinskii-Moriya interaction via chirality dependent atomic-layer stacking, insulator capping and electric field," Sci. Rep. **8**, 1–7 (2018).
[48]B. Zimmermann, W. Legrand, D. Maccariello, N. Reyren, V. Cros, S. Blügel, and A. Fert, "Dzyaloshinskii-Moriya interaction at disordered interfaces from ab initio theory: Robustness against intermixing and tunability through dusting," Appl. Phys. Lett. **113**, 232403 (2018).
[49]V. Kashid, T. Schena, B. Zimmermann, Y. Mokrousov, S. Blügel, V. Shah, and H. G. Salunke, "Dzyaloshinskii-Moriya interaction and chiral magnetism in $3d-5d$ zigzag chains: Tight-binding model and *ab initio* calculations," Phys. Rev. B **90**, 054412 (2014).
[50]H. Yang, A. Thiaville, S. Rohart, A. Fert, and M. Chshiev, "Anatomy of Dzyaloshinskii-Moriya interaction at Co/Pt interfaces," Phys. Rev. Lett. **115**, 267210 (2015).